

# Chapter 21

## Measuring Cell Adhesion Forces: Theory and Principles

Martin Benoit and Christine Selhuber-Unkel

### Abstract

Cell adhesion is an essential prerequisite for survival, communication, and navigation of cells in organisms. It is maintained by the organized binding of molecules from the cell membrane to the extracellular space. This chapter focuses on direct measurements of cellular binding strength at the level of single adhesion molecules. Using atomic force microscopy-based force measurements, adhesion strength can be monitored as a function of adhesion time and environmental conditions. In this way, cellular adhesion strategies like changes in affinity and avidity of adhesion molecules (e.g., integrins) are characterized as well as the molecular arrangement of adhesion molecules in the cell membrane (e.g., molecular clusters, focal adhesion spots, and linkage to the cytoskeleton or tether). Some prominent values for the data evaluation are presented as well as constraints and preparative techniques for successful cell adhesion force experiments.

**Key words:** Cell adhesion, Affinity, Anchoring, Cell membrane, Cytoskeleton, Force measurement, Focal adhesion, Living cells, Force sensor modifications, Clustering

---

### 1. Introduction

Cells are complex microfactories that maintain the basic function of all living organisms. In their lifespan, cells produce huge amounts of distinct biomolecules that they organize within their membrane as well as in the intra- and extracellular space with extreme accuracy. A number of specific tasks are performed using this machinery, such as transducing signals from the extracellular environment and forming responses to these signals.

The cell membrane is central to the interaction of a cell with its environment in that it provides a direct interface between the intra- and extracellular space. Its lipid bilayer incorporates protecting molecules, receptors, ion channels, and adhesion molecules that mediate specific cellular interactions. Adhesion molecules may be

distributed stochastically in the membrane, but they can also appear in the form of clusters at distinct spots. Typically, such clusters are centers for the communication between the intra- and extracellular space which generate special tasks, such as sensing the mechanical properties of the extracellular environment (1–3). An important function of cells is not only to sense forces, but also to actively exert forces (4). This ability is essential to processes, such as cell division, locomotion, and spreading (5, 6). Cellular forces are generated intracellularly by the concerted action of filamentous cytoskeletal elements and molecular motors. In most cell types, the cytoskeleton consists of the actin network, microtubule rods, and other filamentous cell-stiffening molecules. These cytoskeletal elements are not only critical to their role for force generation, but also responsible for the stability of cell shape, the visco-elastic properties of a cell, and stress propagation within a cell and its tissue (7, 8).

Although electron microscopy, NMR, and X-ray diffraction analyses are steadily increasing our knowledge about the structure of extra- and intracellular units and biomolecules, the dynamic properties of biological processes are still unknown to a large extent. Such dynamic processes are ubiquitous. For example, biomolecules act as catalysts, signal amplifiers, gene regulators, energy suppliers, signal transducers, information stores, or transportation units, just to mention a few.

With laser spectroscopy and molecular dynamics simulation, dynamic molecular processes can be visualized at the atomic and femtosecond scale (9). Under equilibrium conditions, the dynamics of molecular interactions are typically studied using calorimetry or surface plasmon resonance techniques and high-resolution fluorescence techniques (10). Importantly, many cellular processes take place under nonequilibrium conditions, (11) such as active intracellular transport processes and enforced binding and unbinding events. These processes can be quantified *in vitro* using nanoscopic techniques, such as optical tweezers (OT) (12, 13), magnetic tweezers (MT) (14, 15), biomembrane-force probe (BFP) (16, 17), or atomic force microscopy (AFM) (18, 19). These techniques typically resolve different force ranges: OT and MT at 0.1–100 pN, BFP at 1–100 pN, and AFM at 5 pN to 100 nN. In order to study the interaction properties of molecules, single-molecule force spectroscopy is commonly used. In these experiments, the interacting molecules typically are isolated from cells, purified, and bound to two opposing surfaces that can be brought into contact with each other. Unfortunately, some molecules cannot easily be extracted from cells and immobilized on surfaces. In particular, most membrane-anchored molecules are not soluble in water and hence are difficult to immobilize without destroying their functionality. Immobilizing such transmembrane proteins in artificial lipid membranes on a substrate provides

a possibility to access membrane protein unbinding events with force spectroscopy; however, this procedure is relatively complicated (20).

An alternative approach to studying interactions of transmembrane proteins is to carry out the adhesion force experiments *in vivo* using living cells. This method is often referred to as “single-cell force spectroscopy.” By binding a complete cell to an AFM cantilever and probing the cellular interactions with the extracellular space, transmembrane proteins can be studied in their native environment, and many of the complexities encountered with bilayer-based studies are bypassed. Cellular receptors are provided in their native conformation by the cell, and the applied force is coupled into the molecules by their “natural handles.” This approach opens a broad field to study cellular mechanisms and strategies that tune the adhesion strength of a cell on the molecular level (21–25).

OT and MT cannot realize such cell-to-cell adhesion measurements, whereas BFP conceptually incorporates red blood cells into the force detection. Even though these techniques have better resolution in the low force regime, only AFM can study the interaction forces between arbitrary cells. AFM also has the advantage of resolving single molecular forces above 5 pN up to multi-molecular interactions in the range of several nanoNewtons.

In this chapter, we focus on single-cell force spectroscopy experiments with AFM, from single-molecule interactions to the interaction of intact cell layers. We first introduce the basic concepts of molecular adhesion, then describe experimental prerequisites and basic experimental methods, and finally present exemplary experiments, which demonstrate the power and limits of using this technique.

---

## 2. Molecular Concepts in Cell Adhesion

Cell adhesion is mediated by membrane-bound cell adhesion molecules (CAMs), for example integrins, cadherins, selectins, and proteins from the Ig-superfamily (26). These transmembrane proteins interact with their extracellular ligands through structural affinity according to the lock-and-key principle, where several weak bonds align to fit the lock and key together, to yield specificity in their interactions. Individual bonds formed during protein–protein interactions, i.e., Van der Waals interactions, hydrophobic interactions, hydrogen bonds, and electrostatic interactions, are several magnitudes weaker than covalent bonds and are continually competing with thermal energy. However, the relative weakness of specific bonds opens many possibilities for cells to easily manipulate the strength of their adhesion.

A parameter that describes the strength of a protein–protein interaction is *affinity*. Affinity is commonly characterized by the dissociation constant  $K_D$  or the off-rate. In force experiments, binding affinity is also represented by the unbinding force and the molecular bond potential (17, 27).

Furthermore, the following strategies can be employed by cells to modulate their adhesion strength:

*Avidity* describes the number of binding competent molecules that are available in the membrane to be accessed by the binding partner. The cell can tune avidity by sterically hiding binding partners behind glycosylations or by modifying the expression level of an adhesion receptor. In some molecules (e.g., integrins), avidity can also be changed by switching the affinity state of the receptor.

*Anchoring* refers to how the adhesion receptor is linked to the cell. Receptors that are freely diffusing in the membrane might reach the adhesion site faster than receptors that are spatially confined by a connection to the cytoskeleton. While a pure lipid anchor (e.g., a ceramide anchor) resists only approximately 20 pN, a transmembrane anchor (e.g., bitopic ( $\alpha$ -helical) transmembrane proteins, polytopic  $\alpha$ -helical proteins, or a transmembrane  $\beta$  barrel) is more resilient with up to approximately 100 pN resistance to failure (28). The strongest group of anchors connects the intracellular domain of transmembrane adhesion receptors to actin, tubulin, or other filaments of the cytoskeleton with binding forces up to the nanoNewton range.

The anchorage of an adhesion molecule defines the mechanical micro-environment of the adhesion molecule in that it controls the lateral motility in the membrane and the loading rate of the applied force to the adhesion site (29). By changing the molecular anchoring, the cell has a wide variety of possibilities to modulate its adhesion state. For example, an adhesion molecule anchored in an actin-rich protrusion (microvillus) exposed on its tip has a higher probability to probe an object near the cell than the one situated within the retracted membrane regions. Also, the binding force of a nonanchored membrane protein is limited to the strength of the membrane anchor, even though the affinity of the binding site might be much stronger. When this type of bond is exposed to external forces, the membrane protein is either ripped out of the membrane or forms a membrane tether (see Fig. 1) depending on the membrane properties. A cell can tune the level of the tether force plateau by the lipid composition and thereby trigger adhesion and de-adhesion processes.

*Clustering* is a strategic combination of avidity, affinity, and anchoring that increases the affinity of an adhesion spot with a strong anchor to the cytoskeleton by forming multimers of binding competent adhesion molecules. Integrin-mediated focal adhesions, the immunological synapse, desmosomes, gap junctions,

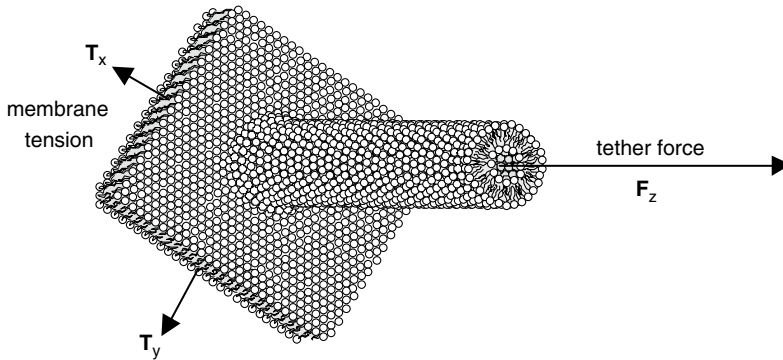


Fig. 1. A tether is a lipid membrane tube that forms due to applied force. The measured tether force consists of the membrane tension via the tube perimeter under static conditions, and pulling at constant velocity generates a viscous and frictional drag force due to rearrangements of membrane molecules at the foot of the tether.

and tight junctions are a few examples of these cell adhesive complexes. In general, adhesion clusters provide a more stable connection than randomly distributed bonds because clusters contain an internal “self-healing mechanism,” where it is possible to rebind broken bonds: bonds which dissociate are not pulled apart because the neighboring molecules in the cluster maintain a close proximity of the interacting surfaces and hence the binding partners (30, 31). With this mechanism, a cluster can withstand forces in the range of several nanoNewtons, i.e., a thousand times more than the strength of a single biomolecular bond.

### 3. Principles of AFM Experiments with Living Cells

#### 3.1. Experimental Prerequisites of Single-Cell Force Spectroscopy

All of the cells use mechanisms to control adhesion strength mentioned in the previous section can be studied with single-cell force spectroscopy. Successful AFM experiments on living cells require control of a few parameters. An AFM that is employed for live cell experiments is ideally set up in conjunction with a light microscope so that the success of cell detachment can be verified optically and the viability of the studied cells can be monitored. In single-cell force spectroscopy experiments, a cell is bound to a cantilever and approached to a surface (see Fig. 3a). Hence, tipless cantilevers should be used in order to prevent harming the cell when it binds to the cantilever. The stiffness of the cantilevers should be chosen according to the studied processes. For example, the cantilevers should be as soft as possible when studying single-molecule interactions on fragile cells.

Furthermore, a highly important parameter for live cell experiments is the sample temperature. Most mammalian cells are optimized to metabolize at 37°C, and the viscosity of the cellular membrane depends strongly on temperature. Particularly, drastic

changes in the viscosity of the cell membrane take place at the transition temperature from liquid to solid phase of the particular lipid bilayer (32). So, it is essential to carry out the AFM experiments at constant temperature under physiological conditions. However, a disadvantage of carrying out an AFM experiment at a temperature other than room temperature is that drift effects are enhanced due to use of a temperature-sensitive force sensor. One solution to this conundrum is to install the whole microscope and AFM head into a heated box and start the experiments when the sample, the cantilever, and the sensor are thermally stabilized.

Suitable functionalization of the cantilever for cell immobilization is also an essential prerequisite for all single-cell force spectroscopy experiments. As the composition of the outer cell membrane can differ greatly from one cell type to the other, coatings normally have to be adapted to each experiment. Several approaches to immobilize cells at the cantilever can be used. A very simple method is to coat the cantilever with lectins (e.g., concanavalin A, wheat germ agglutinin) that bind the glycocalyx of cells (18, 33, 34). A disadvantage of this method is that rupture events between the glycocalyx and the lectin may be mistaken for the actual receptor–ligand ruptures. To circumvent this uncertainty, it is useful to only consider the very last de-adhesion event as a valid measure of the bond of interest. Of course, this analysis requires that the cell is still connected to the cantilever after detachment from the surface. Another solution would be to covalently couple cells to the cantilever, e.g., using glutaraldehyde (35).

In most experimental situations, the interaction between cells and artificial ligand-decorated substrates is studied. In order to avoid nonspecific interaction with the substrate, the surface should be passivated. Furthermore, the ligand should ideally be connected via a soft polymeric spacer so that it can freely rotate in space to explore its surroundings and prevent steric hindrance of binding. As the adhesion ligands on a substrate are exposed to forces, they should also be covalently coupled to this surface. One possible method to covalently immobilize proteins on a glass surface, which is the typical surface used in biological experiments, is to first add a layer of functional silanes (e.g., aminosilane) to the surface and then bind the proteins via bifunctional spacing molecules (e.g., glutaraldehyde or carboxy-PEG) (36–39). This technique also can be used with silicon or silicon nitride surfaces (cantilever tips are commonly made of these materials), and can be applied on gold surfaces by using thiol-functionalized molecules, e.g., alkanethiols, instead of silanes (40). In addition, spacer molecules are typically inserted into the system to avoid nonspecific interactions of the cell with the surface. Many cell types unspecifically bind to most surfaces. In order to avoid the nonspecific binding of the cells, it is important to passivate the substrate. Bovine serum albumin (BSA) is commonly used to inhibit cell and protein

adsorption to surfaces at short timescales. However, BSA often fails to block a surface (41). In such cases, more sophisticated passivation techniques are necessary. In the case of using carboxy-PEG functionalization, one can inactivate the remaining ligand-free carboxyl-groups by ethanolamine leaving behind neutral polyethylene glycol (PEG) groups which prevent protein adsorption due to hydrogen bonding interactions with water. Along the same lines, covalent or electrostatic binding of PEG polymers to the surface can also be used (42, 43). A particularly elegant example is to use poly-L-lysine (PLL)-g-PEG for passivation. This polymer binds with its PLL backbone to negatively charged surfaces, thereby exposing PEG polymers to block nonspecific interactions with the surface. By changing the grafting ratio and length of the PLL and the PEG polymers, respectively, the conformation of the polymer on the surface is precisely controlled (43).

### 3.2. General Features of Cell Adhesion Force Data

Force traces in a cell adhesion experiment are typically highly complex (see Fig. 2). From the force traces, the following parameters can be extracted (34):

The *initial slope* is the initial increase in adhesive force which is approximately linear. After subtracting the spring constant of the cantilever, this parameter basically represents the elastic elements of the cell (see Fig. 5, left arrowhead).

The *maximum adhesion force* indicates the highest force reached in the force plot. This is a rough, first approximation of the adhesion strength.

The *slope prior to a de-adhesion event* gives information on the mechanical properties of the cellular “spacer” (the mechanical

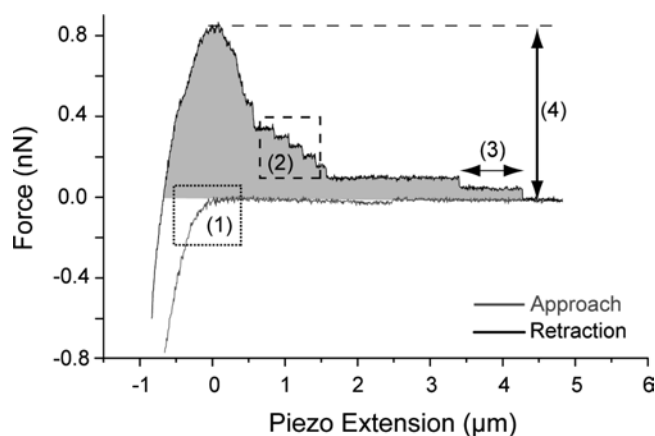


Fig. 2. This representative force–extension curve shows the detachment of a fibroblast (52) cell after 5 s of contact with fibronectin. The *curve* displays the following information: (1) the elastic response of the cell while pressing it to the surface, (2) single-molecule detachment events, (3) the last adhesion event following tether formation, and (4) maximum adhesion force. The *gray area* also represents the work of de-adhesion.

environment anchoring the bond(s) that open at the subsequent de-adhesion event). A slope close to zero indicates that a tether (viscous spacer mostly consisting of cell membrane as described below) has formed, whereas a steep slope results from a stiffer elastic spacer. The slope prior to the last de-adhesion event also defines the loading rate applied to the finally ruptured bond,  $r = dF/dt$ . The loading rate is a highly important parameter for adhesion force measurements because the strength of a biological bond increases logarithmically with increasing loading rate (44). In the force spectroscopy analysis, the bond rupture forces are plotted as a function of loading rate in order to assess the energy landscape of the adhesive interaction.

The *distance* of a de-adhesion event from the original cell surface is a measure for the lifetime  $t$  of a bond, as  $t = \text{distance}/\text{pulling velocity}$ . Determining the distribution of lifetimes provides a means to investigate the kinetics of biological bonds.

The *force step size* of a de-adhesion event can be used as a low-end estimate of the actual unbinding force. While only the very last de-adhesion event is an exact measure of the unbinding force, the de-adhesion events occurring before the last event might be larger, but appear smaller due to force carrying connections still existing (see Fig. 3). These connections could be mediated by nonindependent cellular components bound between surface and cantilever.

The *area* under the force trace has the dimension of energy. It reflects the work of de-adhesion, which is the energy dissipated by the separation of the cell from the surface rather than a summed “adhesion energy” contributed by individual molecular bonds.

The *adhesion probability* cannot be determined by a single force measurement, but requires a set of at least 50 force curves in order to quantify the fraction of force curves with adhesion events.

The *bond formation probability* is determined by the number of recognized adhesion events either per force curve or, in analogy to the adhesion probability, per all detectable single bonds of all force curves (including curves without adhesion) of the whole set of measurements.

*Tethers* (lipid membrane tubes) are a feature often identified in force–extension curves. When a cell tries to adhere, for example a leukocyte in the blood stream, it initially utilizes membrane-anchored weak adhesion molecules. These molecules would detach from the membrane if the adhesion force exceeded the anchorage force of these adhesion molecules. To avoid this phenomenon, cells employ tethers (45), which act similarly to gently releasing fishing line at constant force. In this way, both the force at the binding site and at the anchorage site in the cell membrane is held constant, since cells have a large reservoir of membrane that can be considered unlimited in this case.

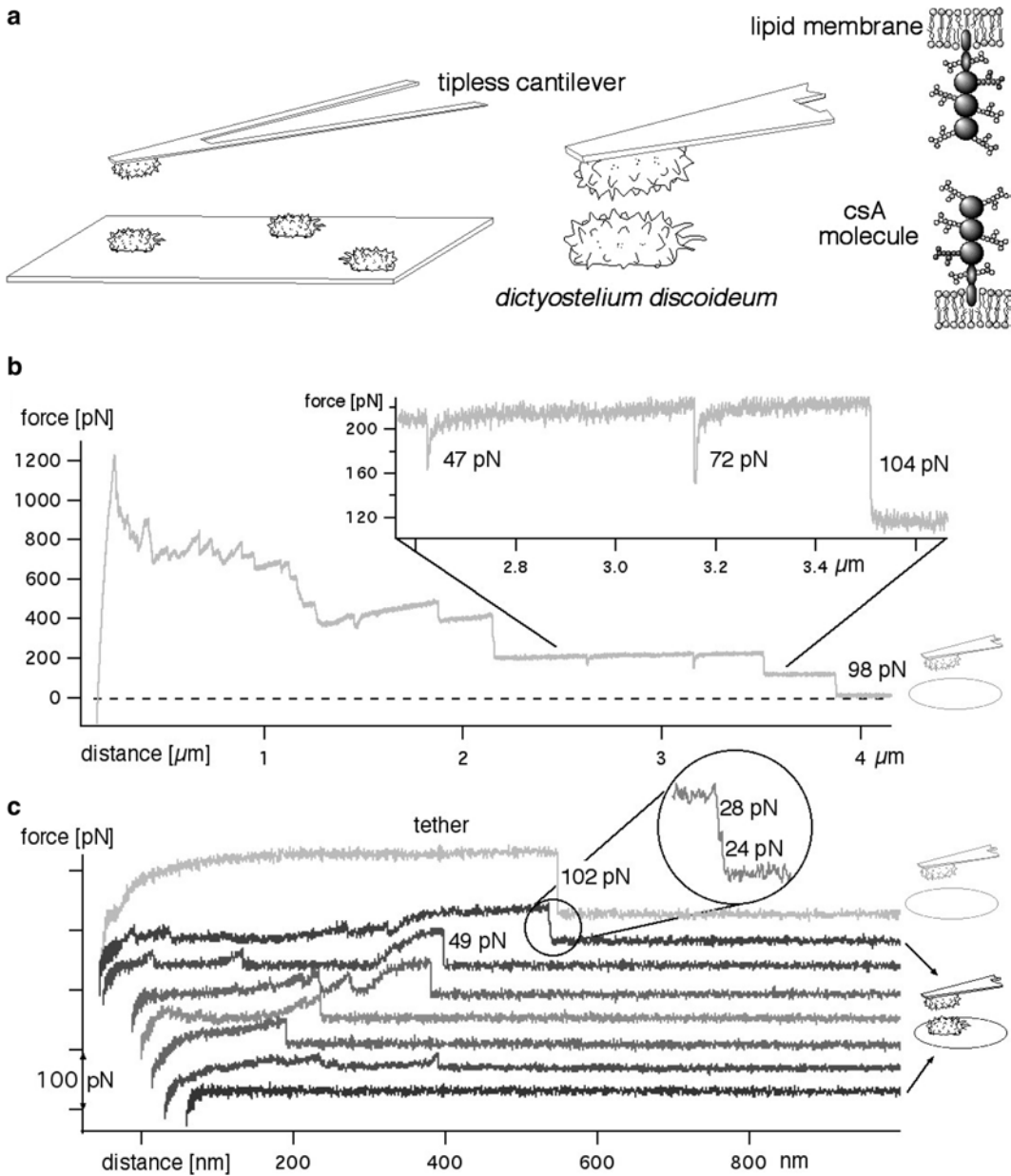


Fig. 3. (a) This schematic presents the basic setup of the experiment and the homophilic interaction of two csA molecules. (b) The force–distance curve for the interaction of *Dictyostelium* with a Petri dish after a contact of 20 s shows strong interaction and large tethers with heights of about 100 pN. The *zoomed inset* shows intermediate de-adhesions that instantly are caught by the same tether. These de-adhesion events show the danger of taking de-adhesion events other than the last event into account, which for sure is not shortened by backup tethers. (c) Superposition of several de-adhesion force traces. They are sorted to show the range of no adhesion (*lowest trace*) to high adhesion forces. The *upper trace* in *gray* was collected from nonspecific adhesion to a Petri dish and displays a typical trace of a single membrane tether. The traces below were collected from csA binding measurements. The *lowest traces* show no tether formation because this process requires more force than one csA bond can hold (csA de-adhesion is the small shark fin pattern with  $23 \pm 7$  pN). *Higher traces* form tethers with at least two bonds in parallel ( $50 \pm 10$  pN). The *zoomed inset* resolves such a twofold bond. Interestingly, the tethers formed on a Petri dish are about 100 pN and have a large variety in plateau force and slope.

A membrane tether (see Fig. 1) forms as a lipid bilayer tube, typically 10–200 nm in diameter, which must counterbalance membrane tension and membrane curvature energies (46–49). The diameter also depends on the composition of lipids and proteins in the membrane, the sample temperature (membrane stiffness), and the amount of molecules (e.g., actin filaments) that are pulled within the tube which also enlarge the tube diameter (50). Interestingly, neurons tend to pull extraordinary tethers up to millimeters in length before detaching (51). Typical forces needed to form a tether range from 10 to 100 pN. Tether failure takes place above 200 pN, depending on the maximum capable membrane tension and the membrane stiffness.

In a force experiment where the cantilever is retracted with constant velocity, a membrane tether can be identified as a nearly constant force plateau in the force trace prior to a detachment event (see Fig. 2, 3, and 5). In this situation, the loading rate of the bond is close to zero and the tether acts as force clamp. When a tether is pulled at constant velocity, a steady flow of lipids into the growing tether is recruited from the cell membrane. This constant force is proportional to the pulling velocity and is determined by friction and viscosity at the origin of the tether on the cell membrane. This growth force exists in addition to the constant force generated by the membrane tension. The maximum membrane tension and bending rigidity of the tether largely depend on the lipid composition and temperature (32, 52, 53). Tethers pulled from cells can vary in diameter and visco-elastic behavior. If actin bundles or membrane proteins are pulled within the tether or if the membrane tension is low, the tether radius can increase to a few hundred nanometers.

---

#### **4. Force Spectroscopy Experiments on Living Cells**

Cells are the smallest units of life. As individuals (single-cell organisms such as amoebae or slime molds), they have adapted very well to the environment during evolution, and in multicellular organisms, they have to adequately react to several environmental changes in order to survive. Hence, a division of labor has been devised, where cells become specialists for certain tasks (e.g., immune cells, neurons, and endothelial cells) in order to provide a better means of adapting to environmental changes or even change the environment. Intercellular communication, differentiation, migration, and many other functions have to be maintained in such a multicellular organism. Therefore, some cellular reactions are universal while some reactions are present only in heart muscle cells, inner ear cells, red blood cells, and so on. Thus, there is no universal protocol for cell adhesion

experiments. In the worst case, a new protocol has to be established for each cell type. Nevertheless, a few basic principles and examples for cell adhesion measurements with AFM are described in the following sections.

#### **4.1. Single Cell-to-Cell Measurements**

The social amoeba *Dictyostelium discoideum* is a highly interesting organism biologically (54, 55). *D. discoideum* is fascinatingly diverse in appearance: if food runs short, the cell switches active genes in the nucleus and changes from a unicellular to a multicellular organism – a slug. During this process, *Dictyostelium* cells meet by a hot spot of a chemokine signal (cAMP) that is sent out from every cell undergoing the change. These switched cells then start to produce a  $\text{Ca}^{2+}$ -independent lipid-anchored glycoprotein in the extracellular membrane called contact site A (csA). During the development of the multicellular *Dictyostelium* slug, csA plays an essential role as the homophilic binding between two csA molecules supports cell aggregation. In order to study this homophilic interaction between two individual csA molecules from different cells, cell–cell adhesion force measurements can be carried out. For studying such single-molecule interactions, the number of other interacting molecules should be as small as possible. One can reduce non-csA binding by removing  $\text{Ca}^{2+}$  from the environment for a few hours prior to the experiment because many adhesion proteins lose their binding function without divalent cations although csA remains active (56). After this treatment, the adhesion probability is typically below 3% (nonspecific interaction) for nonswitched wild-type cells after 0.1 s of cell–cell contact at 100 pN contact force. On the other hand, for csA-expressing *Dictyostelium* cells, the adhesion probability is typically 35% after 0.1 s cell–cell contact at 30 pN contact force. Typical force curves for the separation of interacting *Dictyostelium* cells show a variety of force signals that are received from the same molecular interaction (see Fig. 3).

This variety could be due to the visco-elastic deformation and the plastic activity of the interacting cells causing a significant dissipation of energy. In order to receive the true information about csA–csA binding events, only de-adhesion events from the very last intercellular contact are taken into account in the analysis of adhesion forces (see Fig. 4b, arrowheads).

For the interaction between two individual csA molecules, the adhesion force measurements shown here revealed that the most probable de-adhesion force was 23 pN. The forces varied between 19 pN at loading rates of 20 pN/s and 28 pN at 8 nN/s. After prolonged contacts of 1 and 2 s between two *Dictyostelium* cells, the force histograms showed pronounced force peaks at multiples of 23 pN.

A critical issue when analyzing the measured forces is interpreting where the bond rupture occurs. The csA molecule is

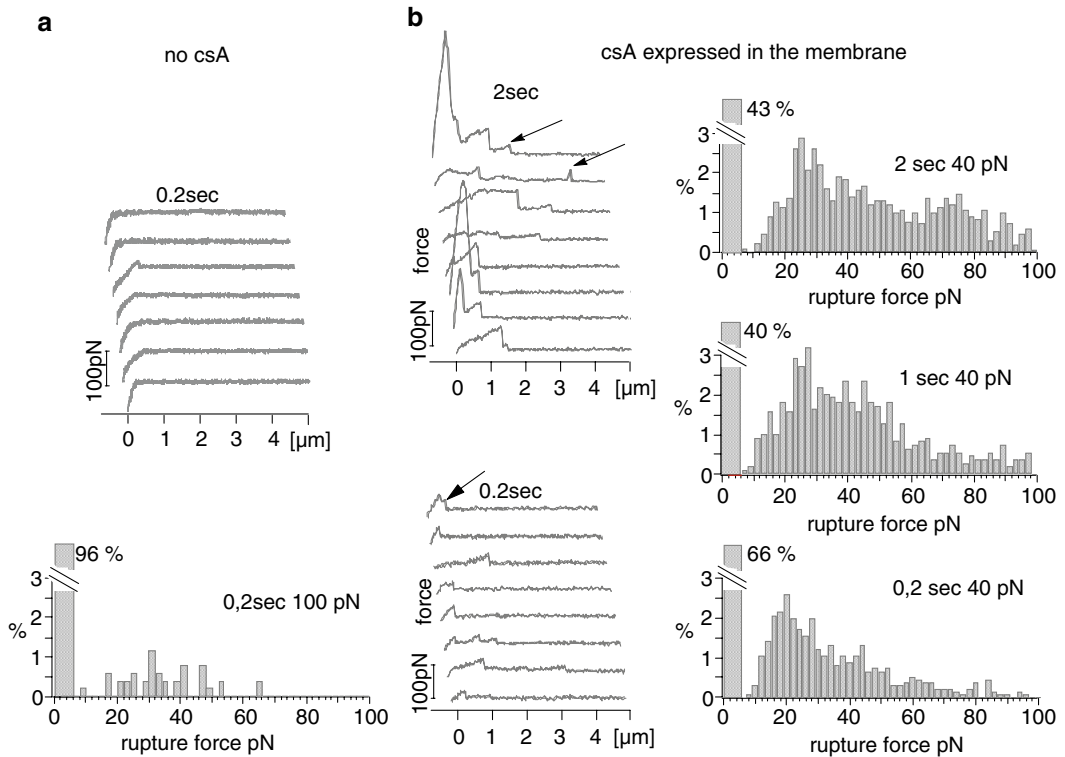


Fig. 4. (a) *Dictyostelium discoideum* in the amoebous state do not express csA molecules, and the remaining intercellular interaction is effectively blocked by the added EDTA. (b) Starved *Dictyostelium* cells express csA, and the adhesion signal of individual interacting csA molecules is measured by the AFM. Arrows on the force traces indicate the last de-adhesion event counted in the histograms. The most probable de-adhesion force is extracted from the histograms (from 20 pN at short contacts to 23 pN for longer contacts). The percentage of *force curves* where no adhesion occurs is indicated by the truncated *bar* to the left side of the histograms. Contact time and contact forces are indicated above the histograms.

known to be only weakly anchored to the cell with a ceramide anchor in the external lipid layer of the membrane. In order to test whether the bond between two csA molecules breaks or if the anchor itself is extracted from the lipid bilayer in an AFM experiment, a genetically modified mutant of *Dictyostelium* expressing csA with transmembrane anchor was employed. In these experiments, no significant change in the adhesion pattern was observed. Therefore, the anchor is believed to be at least as strong as the molecular interaction, and thus csA is extracted from the membrane in less than 50% of the adhesion events (33).

Tether formation is not often observed for csA-mediated *Dictyostelium*-to-*Dictyostelium* adhesion. However, when *Dictyostelium* cells adhere to Petri dishes, tethers dominate the force curves. The pseudopodia-rich surface structure is thought to support tether formation (57). In this case, tethers can also reach lengths of several tens of micrometers and more (see Fig. 3b).

## 4.2. Spheres on Cells

Targeting therapeutic delivery to selected cells within an organism is a desired goal of pharmacology. In particular, designing vehicles loaded with a drug which targets only specific pathogenic cells is a strong aim in medical research. For the design of such vehicles, the molecular composition of the external surface of the vehicle should be specific for binding to a certain type of target cell. Medically relevant particles are often spherical and consist of polymers that are functionalized on the surface. In adhesion force experiments, a small vehicle can be mimicked by a sphere of 5  $\mu\text{m}$  radius, for example, that is immobilized to an AFM cantilever. In order to quantify the interaction with different cell types and to find particle coatings specific for the binding to particular cell types, the initial binding force between the functionalized vehicle and a cell can be quantified. In the experiments described here, the adhesion of cells to two different types of surfaces, positively ( $\text{NH}_2$ ) and negatively ( $\text{COOH}$ ) charged spheres, has been investigated. Two types of breast cancer cell lines were measured in this study, the noninvasive strain MCF-10A and the invasive strain MDA-MB-4355 (58). The analysis of the force traces with respect to adhesion probability and adhesion forces on the single molecular level (while maintained at  $37^\circ\text{C}$  in nutrient medium) showed a higher adhesion probability for the positively charged spheres. This result is likely due to the presentation of a negative net charge by these cells due to expression of carbohydrate groups in the glycocalyx, leading to stronger binding on positively charged spheres.

The most probable “molecular” adhesion force is increased from 20 pN for negatively charged spheres to 25 pN for the positively charged spheres after contacts of 1 ms at 50 pN. Furthermore, an increase in adhesion probability from 20% for negatively charged spheres to almost 80% for positively charged spheres was observed for the MCF-10A cell line compared to an only moderate increase from 30% to almost 50% for the MDA-MB-4355 cell line. Hence, the MCF-10A cells appear much more negatively charged than the MDA-MB-4355 cells.

## 4.3. Cell Layer to Surface Measurements

The examples of cell adhesion force measurements presented so far sought to measure initial adhesion or fast molecular processes on the level of single molecules. These measurements are both important to our understanding of adhesion processes and they are feasible. In contrast, long-term adhesion processes are difficult to measure in a force experiment. For example, cells that initially seem to like a surface might decide to push it away after having explored it for an hour. But how will the adhesion forces involved in binding to artificial bones and implants develop? In this case, it is essential that long-term adhesion is stable and viable. With a bone cell layer on a cantilever, potential implant surfaces can be probed to find out the best surface for durable

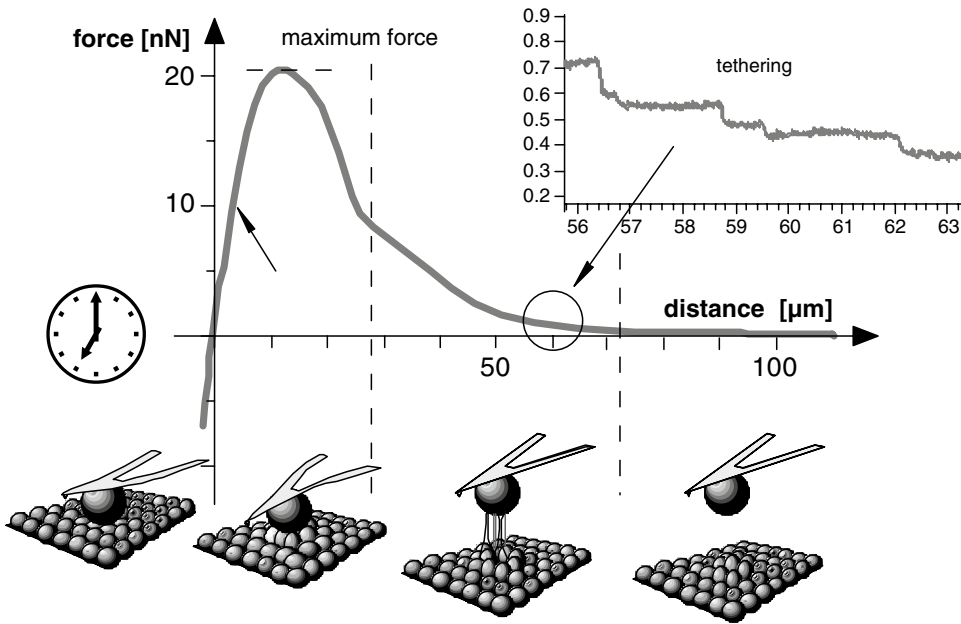


Fig. 5. Schematic series of a fibronectin-coated sphere microfabricated to the cantilever pulled back from a cell layer of epithelial cells (RL cells also described in Fig. 8) after a contact of 20 min (clock symbol) at 5 nN. The corresponding force–distance trace shows a Hookean region (left arrow), the maximum adhesion force, and a descending shoulder consisting of many small force steps (zoomed inset shows the tethering region) from individual molecular interactions.

acceptance of implants by the adhering cells (59). The cell-to-surface contacts can be prolonged to several minutes, maybe up to an hour, but then drift becomes a limiting factor and force spectroscopy is not applicable anymore.

In force experiments with cell layers, the number of cells interacting with the surface is unknown and many adhesion molecules contribute to the force trace in parallel. A typical force graph of a fibronectin-coated sphere mounted to the cantilever after a contact of 20 min at 5 nN on a layer of confluent cells is shown in Fig. 5.

After the contact, an almost Hookean stretching of the cell layer (left arrow) takes place until, by an increasing number of dissociating bonds and the progression of membrane and cytoskeleton disentanglement, the maximum force is reached. The measured maximum adhesion forces are up to three orders of magnitudes higher than in a single molecule experiment. The large maximum adhesion force of 20 nN is the sum of several hundred or thousands of single molecules, each contributing with its weak individual adhesion force. Some of these contributing molecules are still resolved as individual de-adhesion events when zooming into the tethering region in the force traces' descending shoulder. An adhesive interaction length of several tens of micrometers and forces larger than 3 nN, as observed here, is not observed in single-molecule force measurements.

#### 4.4. Cell Adhesion Clusters

The formation of molecular clusters is a ubiquitous mechanism that leads to strong mechanical interactions in cellular systems. Particularly relevant to the adhesion between cells and the extracellular matrix are focal adhesion clusters, often called “focal contacts.” Focal contacts are formed in cells subsequent to the activation and clustering of integrin transmembrane adhesion receptors (60). Integrin activation can be induced by binding to extracellular matrix proteins, such as fibronectin, and in response to integrin activation, further integrin molecules are recruited to the binding site and cluster. After this initial clustering process, a hierarchically organized plaque of intracellular proteins accumulates intracellularly at the integrin cluster. This plaque is also responsible for connecting the integrin cluster with the cellular cytoskeleton. Proteins in the plaque, such as talin, vinculin, and  $\alpha$ -actinin, are very important to these structures because these proteins are supposed to be the first proteins that bind to the early integrin cluster (61, 62).

Focal contacts have many biological functions. For example, they are responsible for a large number of signal transduction events, and they serve as cellular mechanosensors by “feeling” external forces and actively probing the mechanical properties of the cellular environment (3, 63). Due to the complex organization and function of focal contacts, it can be expected that their formation and function rely on a well-defined, hierarchical organization of the proteins in the cluster which is already critical during the initial binding and clustering processes. Hence, it is highly interesting to investigate the requirements necessary for the formation of the initial stages of focal contacts.

Using nanolithographical techniques, it is possible to impose nanometer-sized binding sites for integrins on surfaces. A very elegant method is diblock-copolymer micelle nanolithography. With this method, nanometer-sized gold dots can be arranged in hexagonal patterns on standard glass coverslips, where the spacing between the individual gold dots can be defined between approximately 20 and 400 nm with nanometer precision (64–66). After deposition, the gold dots can be functionalized with thiol-terminated adhesion ligands, e.g., RGD peptides so that they finally serve as nanometer-sized ligand patches for the binding of  $\alpha_v\beta_3$  integrin adhesion receptors (see Fig. 6) (67).

Using these nanostructured surfaces, it has been shown that the extent of integrin-mediated cell spreading and the formation of focal contacts are critically defined by the spacing between RGD ligand patches. In particular, above a ligand patch spacing of approx. 70 nm, cell spreading, proliferation, and focal contact formation are strongly inhibited (71). These results indicate that the molecular binding affinity between the  $\alpha_v\beta_3$  integrin and the RGD is not sufficient for inducing focal contact formation, but their intermolecular spatial arrangement must also fulfill certain requirements.

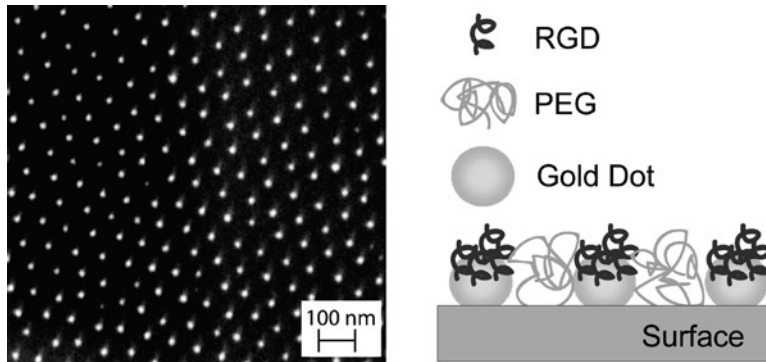


Fig. 6. *Left*: Scanning electron microscope image shows the hexagonal pattern of gold nanodots on a glass surface generated using the block copolymer technique. *Right*: This schematic shows the most likely bio-functionalization pattern of the nanostructured surface used in studies of integrin-mediated adhesion. The polyethylene glycol (PEG) coating prevents nonspecific protein adsorption and cell adhesion to the glass surface, ensuring that the cellular integrins only bind to the gold dots.

In order to study the role of the intermolecular arrangement of integrins and the timescale of the onset of integrin cluster formation, we characterized cell detachment forces as a function of cell adhesion time using an AFM. In the experiments, a fibroblast cell (52) was coupled to a cantilever with concanavalin A and brought into contact with a nanostructured surface for a defined time span between a few seconds to several minutes.

From the experiments, it is immediately clear that nanostructures providing integrin-binding site spacings larger than 60 nm lead to very different detachment forces compared to spacings smaller than 60 nm (see Fig. 7). For 35- and 55-nm integrin-binding site spacing, the detachment forces increase to more than 1 nN within 40 s. For larger spacings, detachment forces do not exceed 500 pN and stay almost constant with adhesion time. This result suggests that cell adhesion is reinforced for spacings smaller than 60 nm, whereas adhesion cannot normally develop for spacings larger than 60 nm (72).

We believe that the observed reinforcement of adhesion results from a cooperative clustering of integrin receptors that can only take place for spacings smaller 60 nm. In a focal contact, the cooperative clustering of integrins is supported by secondary proteins that serve as cross-linkers between the individual integrin molecules. However, if the integrin molecules are located too far apart from each other, such an interconnection might fail to form. Prominent candidates for intracellularly cross-linking integrins are talin (length approx. 60 nm) and  $\alpha$ -actinin (heterodimer length approx. 24 nm). However, biological proof of the involvement of these proteins in the reinforcement of adhesion on RGD nanostructures has not yet been demonstrated.

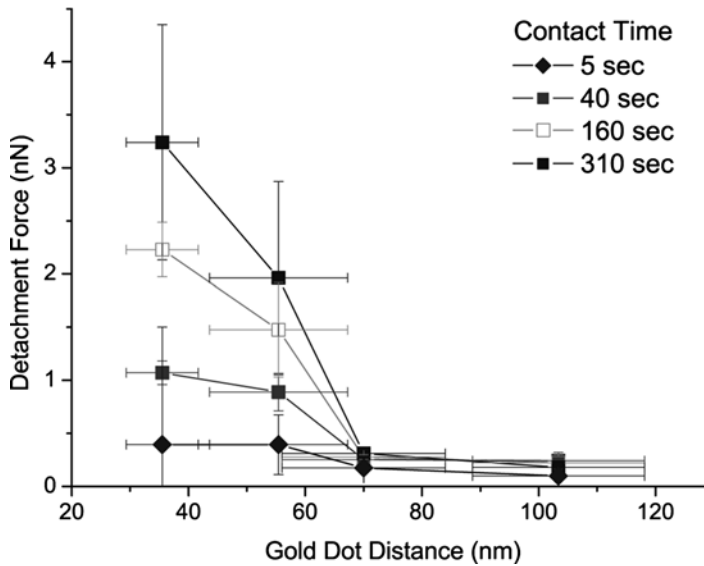


Fig. 7. These results of force versus inter-integrin binding site distance were taken from single-cell force microscopy measurements of fibroblasts on nanostructured surfaces. At 35 and 55 nm integrin binding site spacings, the cell detachment force increases to approximately 1 nN within 40 s of contact. Above 60 nm inter-integrin spacing, the detachment forces increase only slightly with time, and there is no significant difference observed between the forces at 70 and 103 nm. *Error bars* refer to the standard error of the mean.

#### 4.5. Cell Layers on Cell Layers

Experiments between two cell layers present a highly natural cellular environment; however, this situation is extremely complex to analyze. In this layered configuration, cells can polarize, form intercellular connection centers, such as adhesion clusters, and carry out typical habits of epithelial cells. However, in these experiments, neither the surface geometry of the two layers is defined nor can parameters, such as the indentation force and the elasticity of the interacting cells, be calculated. When the two cell layers are brought into contact, they might start to communicate and also establish complex adhesion patterns since thousands of adhesion molecules are contributing to the measured de-adhesion forces (68).

A biological situation where the adhesion between cell layers becomes relevant is the adhesion between trophoblast cells covering the few embryonic cells after fertilization and the uterine epithelial cell layer. In nature, these cells establish the homing of the embryo. For studying this interaction in AFM experiments, the JAR-cell line was used to form the spherical trophoblast cell layer. On a 60- $\mu\text{m}$  sphere, the natural configuration of the trophoblast structure is resembled best in size, shape, and cellular arrangement of the apical region. Receptive uterine epithelial cells (RL95-2 cell line) or nonreceptive uterine epithelial cells (HEC-1-A cell line) were cultured in Petri dishes and resemble either uterine epithelial layer. Both cell layers were held in contact with

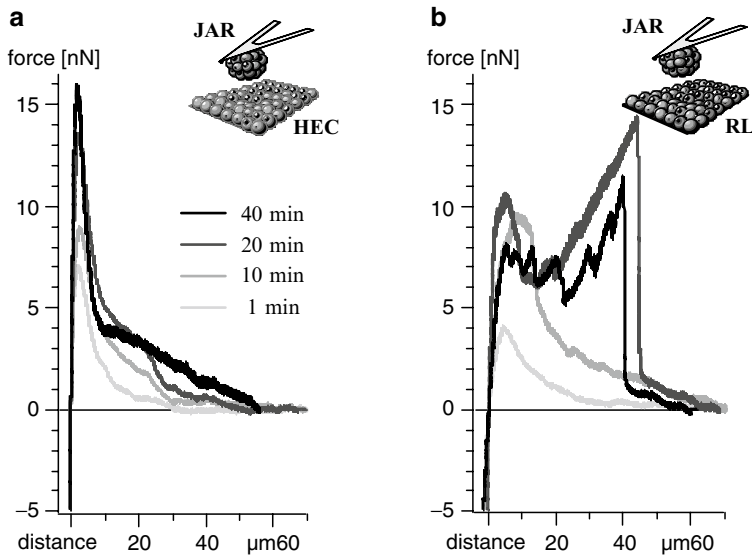


Fig. 8. (a) Representative force traces from nonreceptive HEC cells show increasing maximum adhesion forces with a contact time of 1–40 min after cell layer contact at 5 nN. The individual bonds open sequentially. (b) Representative force traces from receptive RL cells show a similar increase in the maximum adhesion force; however, the work of de-adhesion is drastically increased after 20 min of contact and is marked by strong de-adhesion events after mechanical cell stretching over tens of micrometers.

the trophoblast sphere for several minutes at 5 nN before the cantilever was retracted (see Fig. 8).

An important question for fertilization and pregnancy is how long it would take to firmly arrest the trophoblast layer on either cell layer? When comparing the maximum adhesion forces for trophoblast spheres to HEC or RL cell layers at adhesion times between 1 and 10 min, a stronger adhesion to the HEC cells is observed. Furthermore within 10 min, the adhesion energy dissipation is enhanced for contacts between RL and JAR cell layers. After 20 min, the RL cells firmly connect their adhesion molecules into clusters so that they are strongly connected with the cytoskeleton of the JAR cell layer (69). Importantly, the maximum adhesion force was not able to report this phenomenon, indicating that it is indeed essential to compare different analysis methods in such experiments. Analyzing the force value of the dominating de-adhesion rupture event revealed a force of 15 nN, which suggests this rupture is due to the failure of molecular clusters. From the force measurements of single integrins ( $\alpha_4\beta_1$ ), a typical detachment force appears to be between 20 and 60 pN at loading rates of 10–100 pN/s. Hence, approximately 100–1,000 molecular bonds contribute in the measured clusters. All of these molecules must be connected to the cytoskeleton, or the cluster would separate from the cell and form a tether that breaks at a force of about 300 pN (41).

When checking the viability of the cells after such a strong de-adhesion event, at least one of the cell layers appeared to be severely damaged (cells of either layer were found loosened or even sticking to the opposite layer) so that the experiment cannot be carried out repeatedly as in single-molecule experiments. Although these experiments, therefore, require more preliminary setup time and equipment than single-molecule experiments, the technique provides useful information and quantification for cellular communication between cell layers that would otherwise not be obtained.

---

## 5. Perspectives

In this chapter, we have described the experimental principles of single-cell force spectroscopy and how it can be applied for answering biophysical questions from the level of single molecules to molecular clusters and even multicellular interactions. Although the described experiments may look straightforward at first glance, it is important to remember that each cell might react differently due to the cell cycle, last feeding period, temperature changes during preparation, or the exerted force. Furthermore, a cell as a “spacer” for the molecular bond to be investigated contains several billions of molecules. This complex interplay among all of these factors renders the mechanical characteristics of the cell, since it is the linker between the adhesion molecules and the substrate or the force sensor. Hence, such cell experiments are always associated with experimental and statistical errors, and a large number of experiments must be carried out in order to receive appropriately representative information.

As cells might change their adhesion when reacting to their environment, a cell adhesion experiment can even serve as a reporter for the function of pharmaceuticals (drugs, hormones, and chemokines) that trigger an intracellular reaction which has an impact on adhesion (21). Force spectroscopy can not only characterize antibodies with respect to their interaction force with their specific ligand, but might also identify diseases caused by malfunction of cellular adhesion and optimize related medication.

AFM can also be applied for experiments in electrophysiology. Planar patch-clamp technology turned out to be not only a perfect platform for AFM measurements on non-adherent cells, but also an extension toward simultaneous electrophysiological measurements. This application is extremely attractive for pharmacological research. Here, for example, the mechanical signal from the cell can be correlated in time with activity of membrane pores (70).

In conclusion, AFM experiments on cells are becoming more and more interesting for medical scientists and pharmacists, and many new aspects of cell adhesion might be discovered during the next years.

---

## Acknowledgments

We acknowledge the people involved in the projects described in this chapter, namely, Hermann Gaub, Günther Gerisch, Joachim Spatz, Horst Kessler, Angelika Kardinal, Thomas Nicolaus, and Michael Thie. Furthermore, we thankfully dedicate this chapter to Kristin Michael.

## References

1. Bischofs, I. and Schwarz, U. S. (2003) Cell organization in soft media due to active mechanosensing. *Proc. Natl. Acad. Sci. U. S. A.* **100**, 9274–9279.
2. Discher, D. E., Janmey, P. and Wang, Y.-I. (2005) Tissue Cells Feel and Respond to the Stiffness of Their Substrate. *Science* **310**, 1139–1143.
3. Geiger, B. and Bershadsky, A. (2002) Exploring the Neighborhood: Adhesion-Coupled Cell Mechanosensors. *Cell* **110**, 139–142.
4. Tan, J. L., Tien, J., Pirone, D. M., Gray, D. S., Bhadriraju, K. and Chen, C. S. (2003) From the Cover: Cells lying on a bed of microneedles: An approach to isolate mechanical force. *Proc. Natl. Acad. Sci. U. S. A.* **100**, 1484–1489.
5. Burton, K. and Taylor, D. L. (1997) Traction forces of cytokinesis measured with optically modified elastic substrata. *Nature* **385**, 450–454.
6. Dogterom, M., Kerssemakers, J. W., Romet-Lemonne, G. and Janson, M. E. (2005) Force generation by dynamic microtubules. *Curr. Opin. Cell Biol.* **17**, 67–74.
7. Paul, R., Heil, P., Spatz, J. P. and Schwarz, U. S. (2008) Propagation of Mechanical Stress through the Actin Cytoskeleton toward Focal Adhesions: Model and Experiment. *Biophys. J.* **94**, 1470–1482.
8. Yamada, S., Wirtz, D. and Kuo, S. C. (2000) Mechanics of Living Cells Measured by Laser Tracking Microrheology. *Biophys. J.* **78**, 1736–1747.
9. Puchner, E. M., Alexandrovich, A., Kho, A. L., Hensen, U., Schafer, L. V., Brandmeier, B., Gräter, F., Grubmüller, H., Gaub, H. E. and Gautel, M. (2008) Mechanoenzymatics of titin kinase. *Proc. Natl. Acad. Sci. U. S. A.* **105**, 13385–13390.
10. Vogelsang, J., Cordes, T., Forthmann, C., Steinhauer, C. and Tinnefeld, P. (2009) Controlling the fluorescence of ordinary oxazine dyes for single-molecule switching and superresolution microscopy. *Proc. Natl. Acad. Sci. U. S. A.* **106**, 8107–8112.
11. Mizuno, D., Tardin, C., Schmidt, C. F. and MacKintosh, F. C. (2007) Nonequilibrium Mechanics of Active Cytoskeletal Networks. *Science* **315**, 370–373.
12. Grier, D. G. (2003) A revolution in optical manipulation. *Nature* **424**, 810–816.
13. Mehta, A. D., Rief, M., Spudich, J. A., Smith, D. A. and Simmons, R. M. (1999) Single-Molecule Biomechanics with Optical Methods. *Science* **283**, 1689–1695.
14. Smith, A.-S., Sengupta, K., Goennenwein, S., Seifert, U. and Sackmann, E. (2008) Force-induced growth of adhesion domains is controlled by receptor mobility. *Proc. Natl. Acad. Sci. U. S. A.* **105**, 6906–6911.
15. Walter, N., Selhuber, C., Blümmel, J., Kessler, H. and Spatz, J. P. (2006) Cellular Unbinding Forces of Initial Adhesion Processes on Nanopatterned Surfaces Probed with Magnetic Tweezers. *Nano Lett.* **6**, 398–402.
16. Prechtel, K., Bausch, A. R., Marchi-Artzner, V., Kanteleiner, M., Kessler, H. and Merkel, R. (2002) Dynamic force spectroscopy to probe adhesion strength of living cells. *Phys. Rev. Lett.* **89**, 028101.
17. Merkel, R., Nassoy, P., Leung, A., Ritchie, K. and Evans, E. (1999) Energy landscapes of receptor-ligand bonds explored with dynamic force spectroscopy. *Nature* **397**, 50–53.

18. Grandbois, M., Dettmann, W., Benoit, M. and Gaub, H. E. (2000) Affinity imaging of red blood cells using an atomic force microscope. *J. Histochem. Cytochem.* **48**, 719–724.
19. Rief, M., Gautel, M., Oesterhelt, F., Fernandez, J. M. and Gaub, H. E. (1997) Reversible unfolding of individual titin immunoglobulin domains by AFM. *Science* **276**, 1109–1112.
20. Dewa, T., Sugiura, R., Suemori, Y., Sugimoto, M., Takeuchi, T., Hiro, A., Iida, K., Gardiner, A. T., Cogdell, R. J. and Nango, M. (2006) Lateral organization of a membrane protein in a supported binary lipid domain: direct observation of the organization of bacterial light-harvesting complex 2 by total internal reflection fluorescence microscopy. *Langmuir* **22**, 5412–5418.
21. Schmitz, J. and Gottschalk, K. E. (2008) Mechanical regulation of cell adhesion. *Soft Matter*, 1373–1387.
22. Parot, P., Dufrene, Y. F., Hinterdorfer, P., Le Grimellec, C., Navajas, D., Pellequer, J. L. and Scheuring, S. (2007) Past, present and future of atomic force microscopy in life sciences and medicine. *J. Mol. Recognit.* **20**, 418–431.
23. Ludwig, T., Kirmse, R., Poole, K. and Schwarz, U. S. (2008) Probing cellular microenvironments and tissue remodeling by atomic force microscopy. *Pflugers Arch.* **456**, 29–49.
24. Helenius, J., Heisenberg, C. P., Gaub, H. E. and Muller, D. J. (2008) Single-cell force spectroscopy. *J. Cell. Sci.* **121**, 1785–1791.
25. Selhuber-Unkel, C., Lopez-Garcia, M., Kessler, H. and Spatz, J. P. (2008) Cooperativity in adhesion cluster formation during initial cell adhesion. *Biophys. J.* **95**, 5424–31.
26. Brackenbury, R. (1989) Cell adhesion molecules. *Annu. Rep. Med. Chem.* **25**, 235–244.
27. Oberbarnscheidt, L., Janissen, R. and Oesterhelt, F. (2009) Direct and Model Free Calculation of Force-Dependent Dissociation Rates from Force Spectroscopic Data. *Biophys. J.* **97** L01–03.
28. Oesterhelt, F., Oesterhelt, D., Pfeiffer, M., Engel, A., Gaub, H. E. and Muller, D. J. (2000) Unfolding pathways of individual bacteriorhodopsins. *Science* **288**, 143–146.
29. Schmitz, J., Benoit, M. and Gottschalk, K. E. (2008) The viscoelasticity of membrane tethers and its importance for cell adhesion. *Biophys. J.* **95**, 1448–1459.
30. Erdmann, T. and Schwarz, U. S. (2006) Bistability of cell-matrix adhesions resulting from nonlinear receptor-ligand dynamics. *Biophys. J.* **91**, L60–62.
31. Erdmann, T. and Schwarz, U. S. (2004) Stability of adhesion clusters under constant force. *Phys. Rev. Lett.* **92**, 108102 (DOI: 10.1103/PhysRevLett.92.108102) (<http://prl.aps.org/abstract/PRL/v92/i10/e108102>).
32. Heimburg, T. 2007. Front Matter. In *Thermal Biophysics of Membranes*. Wiley-VCH, Berlin. I–XV.
33. Benoit, M., Gabriel, D., Gerisch, G. and Gaub, H. E. (2000) Discrete interactions in cell adhesion measured by single-molecule force spectroscopy. *Nat. Cell Biol.* **2**, 313–317.
34. Franz, C. M., Taubenberger, A., Puech, P. H. and Muller, D. J. (2007) Studying integrin-mediated cell adhesion at the single-molecule level using AFM force spectroscopy. *Sci STKE* **2007**, pl5.
35. Gladilin, E., Micoulet, A., Hosseini, B., Rohr, K., Spatz, J. and Eils, R. (2007) 3D finite element analysis of uniaxial cell stretching: from image to insight. *Phys. Biol.* **4**, 104–113.
36. Dettmann, W., Grandbois, M., Andre, S., Benoit, M., Wehle, A. K., Kaltner, H., Gabius, H. J. and Gaub, H. E. (2000) Differences in zero-force and force-driven kinetics of ligand dissociation from beta-galactoside-specific proteins (plant and animal lectins, immunoglobulin G) monitored by plasmon resonance and dynamic single molecule force microscopy. *Arch. Biochem. Biophys.* **383**, 157–170.
37. Micoulet, A., Spatz, J. P. and Ott, A. (2005) Mechanical Response Analysis and Power Generation by Single-Cell Stretching. *ChemPhysChem* **6**, 663–670.
38. Stenger, D. A., Georger, J. H., Dulcey, C. S., Hickman, J. J., Rudolph, A. S., Nielsen, T. B., McCort, S. M. and Calvert, J. M. (1992) Coplanar molecular assemblies of amino- and perfluorinated alkylsilanes: characterization and geometric definition of mammalian cell adhesion and growth. *J. Am. Chem. Soc.* **114**, 8435–8442.
39. Kufer, S. K., Puchner, E. M., Gump, H., Liedl, T. and Gaub, H. E. (2008) Single-molecule cut-and-paste surface assembly. *Science* **319**, 594–596.
40. Yousaf, M. N. and Mrksich, M. (1999) Diels-Alder Reaction for the Selective Immobilization of Protein to Electroactive Self-Assembled Monolayers. *J. Am. Chem. Soc.* **121**, 4286–4287.
41. Thie, M., Rospel, R., Dettmann, W., Benoit, M., Ludwig, M., Gaub, H. E. and Denker, H. W. (1998) Interactions between trophoblast and uterine epithelium: monitoring of adhesive forces. *Hum. Reprod.* **13**, 3211–3219.
42. Blümmel, J., Perschmann, N., Aydin, D., Drinjakovic, J., Surrey, T., Lopez-Garcia, M., Kessler, H. and Spatz, J. P. (2007) Protein repellent properties of covalently attached

- PEG coatings on nanostructured SiO<sub>2</sub>-based interfaces. *Biomaterials* **28**, 4739–4747.
43. Pasche, S., Textor, M., Meagher, L., Spencer, N. D. and Griesser, H. J. (2005) Relationship between Interfacial Forces Measured by Colloid-Probe Atomic Force Microscopy and Protein Resistance of Poly(ethylene glycol)-Grafted Poly(L-lysine) Adlayers on Niobia Surfaces. *Langmuir* **21**, 6508–6520.
  44. Evans, E. and Ritchie, K. (1997) Dynamic strength of molecular adhesion bonds. *Biophys. J.* **72**, 1541–1555.
  45. Waugh, R. E. and Hochmuth, R. M. (1987) Mechanical equilibrium of thick, hollow, liquid membrane cylinders. *Biophys. J.* **52**, 391–400.
  46. Marcus, W. D. and Hochmuth, R. M. (2002) Experimental studies of membrane tethers formed from human neutrophils. *Ann. Biomed. Eng.* **30**, 1273–1280.
  47. Raucher, D. and Sheetz, M. P. (1999) Characteristics of a membrane reservoir buffering membrane tension. *Biophys. J.* **77**, 1992–2002.
  48. Harmandaris, V. A. and Deserno, M. (2006) A novel method for measuring the bending rigidity of model lipid membranes by simulating tethers. *J. Chem. Phys.* **125**, 204905.
  49. Sun, M., Graham, J. S., Hegedus, B., Marga, F., Zhang, Y., Forgacs, G. and Grandbois, M. (2005) Multiple membrane tethers probed by atomic force microscopy. *Biophys. J.* **89**, 4320–9.
  50. Hosu, B. G., Sun, M., Marga, F., Grandbois, M. and Forgacs, G. (2007) Eukaryotic membrane tethers revisited using magnetic tweezers. *Phys. Biol.* **4**, 67–78.
  51. Hochmuth, F. M., Shao, J. Y., Dai, J. and Sheetz, M. P. (1996) Deformation and flow of membrane into tethers extracted from neuronal growth cones. *Biophys. J.* **70**, 358–69.
  52. Sackmann, E. 1995. Physical basis of self-organization and function of membranes: physics of vesicles. In *Structure and Dynamics of Membranes*. R. Lipowsky and E. Sackmann, editors. Elsevier, Amsterdam. 213–298.
  53. Seifert, U. and Lipowsky, R. 1995. The morphology of vesicles. In *Structure and Dynamics of Membranes*. R. Lipowsky and E. Sackmann, editors. Elsevier, Amsterdam. 403–463.
  54. Bozzaro, S., Fisher, P. R., Loomis, W., Satir, P. and Segall, J. E. (2004) Guenther Gerisch and Dictyostelium, the microbial model for amoeboid motility and multicellular morphogenesis. *Trends Cell Biol.* **14**, 585–8.
  55. Jin, T. and Hereld, D. (2006) Moving toward understanding eukaryotic chemotaxis. *Eur. J. Cell Biol.* **85**, 905–913.
  56. Beug, H., Katz, F. E. and Gerisch, G. (1973) Dynamics of antigenic membrane sites relating to cell aggregation in *Dictyostelium discoideum*. *J. Cell Biol.* **56**, 647–688.
  57. Gerisch, G. and Weber, I. (2007) Toward the structure of dynamic membrane-anchored actin networks: an approach using cryo-electron tomography. *Cell Adh. Migr.* **1**, 145–148.
  58. Munoz Javier, A., Kreft, O., Piera Alberola, A., Kirchner, C., Zebli, B., Susa, A. S., Horn, E., Kempter, S., Skirtach, A. G., Rogach, A. L., Radler, J., Sukhorukov, G. B., Benoit, M. and Parak, W. J. (2006) Combined atomic force microscopy and optical microscopy measurements as a method to investigate particle uptake by cells. *Small* **2**, 394–400.
  59. Benoit, M. and Gaub, H. E. (2002) Measuring cell adhesion forces with the atomic force microscope at the molecular level. *Cells Tissues Organs* **172**, 174–189.
  60. Cluzel, C., Saltel, F., Lussi, J., Paulhe, F., Imhof, B. A. and Wehrle-Haller, B. (2005) The mechanisms and dynamics of alpha<sub>v</sub>beta<sub>3</sub> integrin clustering in living cells. *J. Cell Biol.* **171**, 383–292.
  61. Geiger, B., Bershadsky, A., Pankov, R. and Yamada, K. M. (2001) Transmembrane extracellular matrix-cytoskeleton crosstalk. *Nat. Rev. Mol. Cell Biol.* **2**, 793–805.
  62. Zaidel-Bar, R., Itzkovitz, S., Ma'ayan, A., Iyengar, R. and Geiger, B. (2007) Functional atlas of the integrin adhesome. *Nat. Cell Biol.* **9**, 858–867.
  63. Vogel, V. and Sheetz, M. (2006) Local force and geometry sensing regulate cell functions. *Nat. Rev. Mol. Cell Biol.* **7**, 265–275.
  64. Haupt, M., Miller, S., Ladenburger, A., Sauer, R., Thonke, K., Spatz, J. P., Riethmüller, S., Möller, M. and Banhart, F. (2002) Semiconductor nanostructures defined with self-organizing polymers. *J. Appl. Phys.* **91**, 6057–6059.
  65. Glass, R., Möller, M. and Spatz, J. P. (2003) Block copolymer micelle nanolithography. *Nanotechnology* **14**, 1153–1160.
  66. Spatz, J. P., Mößner, S., Hartmann, C., Möller, M., Herzog, T., Krieger, M., Boyen, H., Ziemann, P. and Kabius, B. (2000) Ordered Deposition of Inorganic Clusters from Micellar Block Copolymer Films. *Langmuir* **16**, 407–415.
  67. Wolfram, T., Belz, F., Schoen, T. and Spatz, J. P. (2007) Site-specific presentation of single recombinant proteins in defined nanoarrays. *Biointerphases* **2**, 44–48.
  68. Pierres, A., Prakasam, A., Touchard, D., Benoliel, A. M., Bongrand, P. and Leckband, D.

- (2007) Dissecting subsecond cadherin bound states reveals an efficient way for cells to achieve ultrafast probing of their environment. *FEBS Lett.* **581**, 1841–1846.
69. Thie, M., Herter, P., Pommerenke, H., Dürr, F., Sieckmann, F., Nebe, B., Rychly, J. and Denker, H.-W. (1997) Adhesiveness of the free surface of a human endometrial monolayer as related to actin cytoskeleton. *Mol. Hum. Reprod.* **3**, 275–283.
70. Pamir, E., George, M., Fertig, N. and Benoit, M. (2008) Planar patch-clamp force microscopy on living cells. *Ultramicroscopy* **108**, 552–557.
71. Arnold, M., Cavalcanti-Adam, A., Glass, R., Blümmel, J., Eck, W., Kessler, H., and Spatz, J. P. (2004) Activation of integrin function by nanopatterned adhesive interfaces, *Chem. Phys. Chem.* **3**, 383. (<http://onlinelibrary.wiley.com/doi/10.1002/cphc.200301014/abstract>).
72. Selhuber-Unkel, C., López-García, M., Kessler, H., and Spatz, J. P. (2008) Cooperativity in adhesion cluster formation during initial cell adhesion. *Biophys. J.* **95**, 5424–5431. ([http://www.cell.com/biophysj/abstract/S0006-3495\(08\)78965-3](http://www.cell.com/biophysj/abstract/S0006-3495(08)78965-3)].